Spectrochimica Acta Part A 76 (2010) 496–501

Contents lists available at ScienceDirect

Spectrochimica Acta Part A: Molecular and Biomolecular Spectroscopy

journal homepage: www.elsevier.com/locate/saa

Synthesis, characterization and biological study on Cr^{3+}, ZrO^{2+}, HfO^{2+} and UO_2^{2+} complexes of oxalohydrazide and bis(3-hydroxyimino)butan-2-ylidene)-oxalohydrazide

A.A. El-Asmy*, O.A. El-Gammal, H.A. Radwan

Chemistry Department, Faculty of Science, Mansoura University, Mansoura, Dakhalia 35516, Egypt

ARTICLE INFO

Article history:
Received 6 December 2009
Received in revised form 20 March 2010
Accepted 14 April 2010

Keywords:
Oxalohydrazide
Oxalyl bis(diacetylmonoxime hydrazone)
Cr^{3+}, ZrO^{2+}, HfO^{2+} and UO_2^{2+} complexes

ABSTRACT

Cr^{3+}, ZrO^{2+}, HfO^{2+} and UO_2^{2+} complexes of oxalohydrazide (H_2L^1) and oxalyl bis(diacetylmonoxime hydrazone) [its IUPAC name is oxalyl bis(3-hydroxyimino)butan-2-ylidene)oxalohydrazide] (H_4L^2) have been synthesized and characterized by partial elemental analysis, spectral (IR; electronic), thermal and magnetic measurements. $[Cr(L^1)(H_2O)_3(Cl)]\cdot H_2O$, $[ZrO(HL^1)_2]\cdot C_2H_5OH$, $[UO_2(L^1)(H_2O)_2]$ $[ZrO(H_3L^2)(Cl)]_2\cdot 2H_2O$, $[HfO(H_3L^2)(Cl)]_2\cdot 2H_2O$ and $[UO_2(H_2L^2)]\cdot 2H_2O$ have been suggested. H_2L^1 behaves as a monobasic or dibasic bidentate ligand while H_4L^2 acts as a tetrabasic octadentate with the two metal centers. The molecular modeling of the two ligands have been drawn and their molecular parameters were calculated. Examination of the DNA degradation of H_2L^1 and H_4L^2 as well as their complexes revealed that direct contact of $[ZrO(H_3L^2)(Cl)]_2\cdot 2H_2O$ or $[HfO(H_3L^2)(Cl)]_2\cdot 2H_2O$ degrading the DNA of Eukaryotic subject. The ligands and their metal complexes were tested against Gram's positive Bacillus thuringiensis (BT) and Gram's negative (*Escherichia coli*) bacteria. All compounds have small inhibitory effects.

© 2010 Elsevier B.V. All rights reserved.

1. Introduction

The synthesis and structural characterization of hydrazone complexes have recently developed to compare their coordinative behavior with their antimicrobial activities. Hydrazones of pyridoxal phosphate and its analogous have been studied to understand the mechanism of action for vitamin B_6-containing enzymes [1]. A series of pyridazinyl hydrazones were found to inhibit tyrosine hydroxylase and dopamine-hydroxylase *in vivo* and *in vitro* [2]. Tridentate hydrazones have been evaluated as potential oral iron-chelating drugs for genetic disorders such as thalassemia [3]. It was noted that salicylaldehydebenzoyl hydrazone (H_2Sb) is unusually potent inhibitor of DNA synthesis and cell growth in a variety of human and rodent cell lines [4]. Testing of $[Cu(HSb)Cl]\cdot H_2O$ showed a significant increase in potency when compared with the free ligand leading to the suggestion that the metal complexes are more biologically active than the free ligand. Compounds containing oxime and amino groups were used as analytical reagents for the micro-determination of some transition metal ions and as ion exchange resins [5]. Previous papers [6–11] were reported on some oxime hydrazone complexes. Binuclear complexes of oxalyl bis(diacetylmonoxime hydrazone) suggested an octahedral geometry for the VO^{2+} complex, tetrahedral for the Zn(II) and square planar for Co(II), Ni(II) and Cu(II) complexes. The *in vitro* antimicrobial activity of the investigated compounds revealed a higher activity of the ligand than its complexes [12]. The antimicrobial properties of polyesters containing Schiff-base metal complexes were investigated against selected microorganisms and was found higher than the standard drugs [13].

Up to my knowledge, no work was done on the complexes containing Cr^{3+}, ZrO^{2+}, HfO^{2+} and UO_2^{2+} ions with oxalohydrazide and oxalyl bis(diacetylmonoxime hydrazone).

2. Experimental

$CrCl_3\cdot 3H_2O$, $ZrCl_4$, $HfCl_4$ and $UO_2(OAc)_2$, diethyl oxalate, hydrazine hydrate, diacetylmonoxime, ethanol, diethyl ether, DMF and DMSO were of pure chemical grade and obtained from the BDH chemicals.

2.1. Synthesis of the ligands

Oxalohydrazide $(NH_2NHCO)_2$ and oxalyl bis(diacetylmonoxime hydrazone) [IUPAC name: bis(3-hydroxyimino)butan-2-ylidene)-oxalohydrazide] were prepared as previously reported [14,12]. The purity was checked by melting point and thin layer chromatography (TLC).

* Corresponding author. Tel.: +20 101645966; fax: +20 502236787.
E-mail address: aelasmy@yahoo.com (A.A. El-Asmy).

1386-1425/$ – see front matter © 2010 Elsevier B.V. All rights reserved.
doi:10.1016/j.saa.2010.04.012

2.2. Preparation of the complexes

In the preparation of zirconyl and hafnyl complexes, the calculated amounts of zirconium tetrachloride heptahydrate or hafnium tetrachloride were dissolved in bidistilled water to give their oxysalts. In the preparation of H_2L^1 complexes, the calculated amount (1.18 g; 0.01 mol) of the ligand was dissolved in 20 mL bidistilled water and then mixed with equimolar amount (0.01 mol) of zirconyl chloride, chromium chloride or uranyl acetate in bidistilled water. The reaction mixture was heated under reflux on a water bath for 4–6 h. For H_4L^2 complexes, 0.057 g (0.005 mol) of the ligand was dissolved in 30 mL EtOH and mixed with the amount of zirconyl, hafnyl, chromium chlorides, or uranyl acetate salts (0.005 mol) dissolved in 10 mL bidistilled water.

All the reaction mixtures were heated under reflux on a water bath for 2–6 h. The resulting solid complexes were filtered immediately while the solution was still hot, washed with ethanol followed by diethyl ether and dried in a vacuum desiccator over anhydrous $CaCl_2$.

2.3. Antibacterial and genotoxicity studies

The organic ligands and their metal complexes were screened for their antimicrobial activity using Gram's positive Bacillus thuringiensis (BT) and Gram's negative bacteria (*Escherichia coli*). The media prepared for bacteria were as reported earlier [15]. For a genotoxicity study, a solution of 2 mg of calf thymus DNA was dissolved in 1 mL of sterile distilled water where the investigated ligand and its complexes were prepared by dissolving 2 mg/mL DMSO. An equal volume of each compound and DNA were mixed thoroughly and kept at room temperature for 2–3 h. The effect of the compounds on the DNA was analyzed by agarose gel electrophoresis. A 2 μl of loading dye were added to 15 μl of the DNA mixture before being loaded into the well of an agarose gel. The loaded mixtures were fractionated by electrophoresis, visualized by UV and photographed.

2.4. Equipment

The IR spectra were recorded as KBr disc on a Mattson 5000 FTIR Spectrophotometer. The UV–vis. spectra of the complexes were recorded on UV_2 Unicam Spectrophotometer. The magnetic measurements were carried out on a Johnson Matthey magnetic balance, UK. Thermogravimetric measurements were recorded on a DTG-50 Shimadzu thermogravimetric analyzer. The nitrogen flow and heating rate were 20 mL min^{-1} and 10 °C min^{-1}, respectively. The molecular geometry of the ligands is first optimized and the Semi-empirical method PM3 is then used for optimizing the full geometry of the system using Polak–Ribiere (conjugate gradient) algorithm and unrestricted Hartee–Fock (UHF) is employed keeping RMS gradient of 0.01 kcal/Å mol.

2.5. Analyses

Carbon, hydrogen and nitrogen contents of the ligands and their complexes were determined at the Microanalytical Unit of Cairo University, Egypt. Zirconium was determined according to Marczenko method [16]. A solution containing 30 μg of ZrO^{2+} sample was placed in a 25 mL standard measuring flask and diluted with bidistilled water. One mL of this solution was added to 1 mL of ascorbic acid solution and 1 mL of xylenol orange indicator and diluted with 0.6 M HCl to the mark. It mixed well and allowed to stand for 10 min. The absorbance of the solution was measured at 535 nm using 1% aqueous solution of ascorbic acid as a standard. Chromium was determined as described in Vogel [17]: 20 μg of Cr(III) complex was evaporated with little amount of H_2SO_4. The residue was cooled and 3–4 drops of $KMnO_4$ were added. The beaker was covered with a glass watch and heated gently for 15 min. Sodium azide solution was added drop wise. The solution was cooled and transferred to 25 mL standard measuring flask, and 1 mL of diphenylcarbazide solution was added and completed to the mark with bidistilled water. The solution was stirred thoroughly and the absorbance was measured at 545 nm using water as a reference. 0.1 g of uranyl complex was placed in a clean and dry weighed crucible and ignited on bunzen flame for 15 min. After that, the crucible was ignited in a muffle at 1000 °C to constant weight for 2 h. The residue was cooled and weighed again as U_3O_8.

3. Results and discussion

Elemental analysis, yield and color of the complexes formed between oxalohydrazide (H_2L^1) or oxalyl bis(diacetylmonoxime hydrazone) (H_4L^2) and Cr^{3+}, ZrO^{2+}, HfO^{2+} or UO_2^{2+} are summarized in Table 1. The results confirm the formulae $[ZrO(HL^1)_2]\cdot C_2H_5OH$, $[Cr(L^1)(Cl)(H_2O)_3]$, $[UO_2(L^1)(H_2O)_2]$, $[ZrO(H_3L^2)(Cl)]_2\cdot 2H_2O$, $[HfO(H_3L^2)(Cl)]_2\cdot 2H_2O$ and $[UO_2(H_2L^2)]\cdot 2H_2O$. The complexes are insoluble in most common organic solvents. The partial solubility of the complexes in DMSO or DMF prevents the measurements of their molar conductances. They are thermally stable and have high melting points (>300 °C). All complexes are diamagnetic as revealed from their complete or incomplete d- or f-orbitals, except of the Cr^{3+} complex which measures 4.9 B.M. The electronic spectra showed charge transfer bands which are the main reason for the intense color of the complexes.

3.1. IR and electronic spectra

3.1.1. IR spectra of H_2L^1 and its complexes

The IR spectrum of H_2L^1 showed bands at 3291, 3253, 3195, 1685, 1535, 1272 and 977 cm^{-1} assignable to $\upsilon_{as}(NH_2)$, $\upsilon_s(NH_2)$, υ(NH), υ(C=O) and amide (III and IV) group, respectively (Table 2).

In the IR spectrum of $[ZrO(HL^1)_2]\cdot C_2H_5OH$, the υ(C=O) band appeared weak indicating that one of the carbonyl groups participates in coordination by removing the amide proton ($HNC{=}O \rightarrow N{=}C{-}O^-$) while the other group still uncoordinated; the weak band at 490 cm^{-1} is assigned to υ(M–O). The shoulder at 1633 cm^{-1} assigned to υ(C=N) is due to the enolization of NHCO group. The broad multiple bands at 3461–3289 may include the υ(OH) of ethanol, the υ(NH) and the NH_2 vibrations. Evidence for participation of NH_2 comes from the shift of the 1618 cm^{-1} band in the ligand to 1563 cm^{-1} in the complex. The new strong band at 1020 cm^{-1} is due to υ(Zr=O). All these observations suggest the monobasic bidentate (C–O and NH_2) nature of H_2L^1 in this complex.

In $[Cr(L^1)(H_2O)_3(Cl)]H_2O$ and $[UO_2(L^1)(EtOH)_2]$, the ligand behaves as a dibasic bidentate coordinating *via* the two carbonyl groups (enolic form). This mode of chelation is confirmed by the complete disappearance of υ(C=O) and υ(NH) with the appearance of a new band at 1620–1633 cm^{-1} due to υ(C=N*). The new band is found strong due to its overlap with $\delta(NH_2)$. The $\upsilon(NH_2)$ bands appear broad centered at 3246 cm^{-1} more or less at the same position as in the ligand spectrum confirming its non-coordination. Further support for the enolization is the appearance of a strong band at 1308 cm^{-1} due to υ(C–O). In $[Cr(L)(H_2O)_3Cl]H_2O$, the two new bands at 601 and 551 cm^{-1} are due to $\upsilon(M{-}OH_2)$ [18]. The ^1H NMR spectrum of $[UO_2(L)(EtOH)_2]$ in DMSO-d_6 showed the NH_2 protons at 7.89 ppm. The signals at 2.79 and 1.75 may be due to the CH_3 and CH_2 of ethanol. Scheme 1 shows the proposed geometry of $[UO_2(L^1)(EtOH)_2]$.

3.1.2. Electronic spectra of H_2L^1 and its complexes

The UV spectrum of H_2L^1 showed bands at 43,860 and 42,020 due to the $\pi \rightarrow \pi^*$ and $n \rightarrow \pi^*$ transitions of the C=O

Table 1
Color, melting points, yields and partial elemental analyses of the ligands and their complexes.

Compound, formula (formula weight)	Color	Yield (%)	%Found (calcd.)				
			C	H	M	N	Cl
H_2L^1	White	84	19.9	5.4 (5.1)	–	47.1	–
$C_2H_6N_4O_2$ (118.110)			(20.3)			(47.4)	
$[Cr(L^1)(H_2O)_3(Cl)]H_2O$	Pale green	76	9.0	3.9 (4.3)	19.1 (18.8)	19.9	13.3
$C_2H_{12}N_4O_6ClCr$ (275.59)			(8.7)			(20.3)	(12.8)
$[ZrO(HL^1)_2]\cdot C_2H_5OH$	Yellowish orange	81	19.0	3.9	27.3	–	
$C_6H_{16}N_8O_6Zr$ (387.39)			(18.6)	(4.2)	(27.6)		–
$[UO_2(L^1)(EtOH)_2]$	Yellow	89	14.2 (14.2)	2.4 (2.4)	47.4	–	
$C_4H_{12}N_4O_6U$ (506.26)					(47.0)		–
H_4L^2	White	67	42.3	6.0	–	29.3	–
$C_{10}H_{16}N_6O_4$ (284.29)			(42.2)	(5.7)		(29.6)	
$[ZrO(H_3L^2)(Cl)]_2\cdot 2H_2O$	Yellow	80	27.5	3.6	24.0	18.6	7.9
$C_{20}H_{34}N_{12}O_{12}Cl_2Zr_2$ (887.82)			(27.1)	(3.9)	(24.1)	(18.9)	(8.0)
$[HfO(H_3L^2)(Cl)]_2\cdot 2H_2O$	Yellowish orange	71	21.6	3.4	–	15.1	6.1
$C_{20}H_{34}N_{12}O_{12}Cl_2Hf_2$ (1097.86)			(21.9)	(3.4)		(15.3)	(6.5)
$[UO_2(H_2L^2)]\cdot 2H_2O$	Yellow	85	21.3	3.2	41.2	14.3	–
$C_{10}H_{18}N_6O_9U$ (571.33)			(21.0)	(3.2)	(41.6)	(14.7)	

Table 2
Assignments of the IR spectral bands of H_2L^1 and its complexes.

Compound	$\upsilon(H_2O)$ or υ(OH)	$\upsilon_{as}(NH_2)\upsilon_s(NH_2)$	υ(NH)	υ(C=O)	$\delta(NH_2)$	υ(C=N)[a]	υ(M–O)
H_2L^1	–	3291(s) 3253(m)	3195(m)	1685 (s)	1618(s)	–	–
$[ZrO(HL^1)_2]\cdot C_2H_5OH$	3461(br)	3289(sh) 3250(sh)	3127(w)	1687 (w)	1563(w)	1633(m)	1020(s)
$[Cr(L^1)(Cl)(H_2O)_3]H_2O$	3421(br)	3290(sh) 3250(sh)	–	–	1633(w)	1633(m)	601[a](m) 551(m)
$[UO_2(L^1)(EtOH)_2]$	3417 (br)	3290(sh) 3250(sh)	–	–	1620(s)	1620(s)	942(s) 810(m)

S = strong; m = medium; w = weak; sh = shoulder; br = broad
[a] This band may be due to υ(Cr–OH_2).

Table 3
Electronic spectral data of the ligands and their complexes.

Compound	State	Intraligand and charge transfer (cm^{-1})
H_2L^1	DMF	43860, 42020
$[ZrO(HL^1)_2]\cdot C_2H_5OH$	Nujol	33110, 26178
$[Cr(L^1)(Cl)(H_2O)_3]H_2O$	DMF	32895, 25320, 23920, 17545
$[UO_2(L^1)(EtOH)_2]$	DMSO	36230, 32155, 24630, 9230, 18050
H_4L^2	DMF	48540, 45450, 43470, 39210, 36495, 4480
$[ZrO(H_3L^2)(Cl)]_2\cdot 2H_2O$	DMF	35460, 33785, 26455, 24270
$[HfO(H_3L^2(Cl)]_2\cdot 2H_2O$	DMF	26520, 25780, 24330, 22220, 21190

group (Table 3). $[ZrO(HL^1)_2]\cdot C_2H_5OH$ showed bands at 33,110 and 26,180 cm^{-1} which could be assigned to the intraligand and charge transfer transitions. The electronic spectrum of $[Cr(L^1)(H_2O)_3Cl]\cdot H_2O$ showed strong absorption bands at 17545 (υ_1), 23920 (υ_2) and 25320 (υ_3) due to the $^4A_{2g}(F) \rightarrow {}^4T_{2g}$ (F) (υ_1), $^4A_{2g}(F) \rightarrow {}^4T_{1g}(F)$ (υ_2) and $^4A_{2g}(F) \rightarrow {}^4T_{1g}(P)$ (υ_3), transitions, respectively. The υ_1 transition is a direct measure of 10 Dq. The

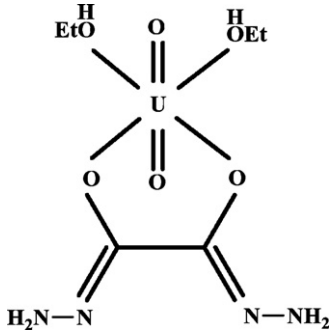

Scheme 1. Structure of $[UO_2(L^1)(EtOH)_2]$.

values of B and β can be calculated applying the equation [19]: $B' = (2 \times \upsilon_1{}^2) - 3 \times \upsilon_1 \times \upsilon_2 + \upsilon_2{}^2/15\ \upsilon_2 - 27\upsilon_1$, $\beta = B'/B$, where B is the electronic repulsion reported for the free metal ion. It is found that 10 Dq = 17,544 cm^{-1}, B = 620 cm^{-1} and β = 0.67. In addition, the μ_{eff} value (4.9 B.M) is in the range reported for the Cr(III) octahedral geometry.

In the electronic spectrum of $[UO_2(L^1)(EtOH)_2]$, the band at 24,630 cm^{-1} is assigned to the $^1\Sigma g^+ \rightarrow {}^3\pi_4$ transition similar to the OUO symmetric stretching frequency for the first excited state [20] while that at 26,040 cm^{-1} is assigned to a charge transfer transition, probably O → U.

3.1.3. IR spectra of H_4L^2 and its complexes

The IR spectrum of H_4L^2 showed bands at 3395, 3305, 1695, 1602, 1508, 1430 and 1004 cm^{-1} attributed to $\nu(OH)_{oxime}$, ν(NH), ν(C=O), $\nu(C{=}N)_{hydrazone}$, amide II, $\nu(C{=}N)_{oxime}$ and ν(NOH), respectively (Table 4).

In the IR spectra of $[ZrO(H_3L^2)(Cl)]_2\cdot 2H_2O$; $[HfO(H_3L^2)(Cl)]_2\cdot 2H_2O$ and $[UO_2(H_2L^2)]_2\cdot 2H_2O$, the ligand coordinates to the two metal centers as a dibasic tetradentate through the four azomethine nitrogen's (oxime and hydrazone). This confirmed through the shift of $\nu(C{=}N)_{hydrazone}$ and $\nu(C{=}N)_{oxime}$

Table 4
Assignments of the IR spectral bands of H_4L^2 and its complexes.

Compound	$\nu(OH)_{oxime}$	$\nu(N–H)$	$\nu(C{=}O)$	$\nu(C{=}N)_{hyd}$	$\nu(C{=}N)_{oxime}$
H_4L^2	3396(s)	3305(s)	1695(s)	1602(w)	1430(s)
$[ZrO(H_3L^2)(Cl)]_2{\cdot}2H_2O$	3410(br)	3310(br)	1686(s)	1586(w)	1414(s)
$[HfO(H_3L^2)(Cl)]_2{\cdot}2H_2O$	3402(m)	3304(m)	1695(s)	1590(sh)	1425(m)
$[UO_2(H_2L^2)]{\cdot}2H_2O$	3416[a](br)	3340(sh)	1650(s)	1571(s)	1426(m)

[a] ν(O–H) of water.

to (1586, 590); (1414, 1425) and (1426, 1571) cm^{-1} with lowering of their intensity. The disappearance of $\nu(OH)_{oxime}$ in $[UO_2(H_2L^2)]_2{\cdot}2H_2O$ with the appearance of a broad band due to the hydrated water. Also, the weakness of $\nu(NOH)_{oxime}$ confirming the participation of $C{=}N_{oxime}$ in coordination; the result is supported by a new band at 488 and 492 cm^{-1} assigned to ν(M–N) in the two complexes. The ν(Hf=O) band is observed at 794 cm^{-1}. The broadness and weakness of $\nu(OH)_{oxime}$ confirm the deprotonation of one hydroxyl group and the existence of the second uncoordinated. The carbonyl band is more or less unshifted.

The ^1H NMR spectrum of $[UO_2(H_2L^2)]_2{\cdot}2H_2O$ showed no signals for the OH protons. The NH signals appear at δ = 10.2 ppm. The methyl groups appear at δ = 2.81 and 2.50 ppm.

The investigated uranyl complexes of the two ligands exhibit bands at 926–942 and 810–869 cm^{-1} assigned to the υ_3 and υ_1 vibrations, respectively, of the dioxouranium ion [21]. The value of υ_3 is used to calculate the force constant (F) of (O=U=O) by the method of McGlynn and Smith [22]: $(\nu_3)^2 = (1307)^2\ (F_{U-O})/14.103$. The force constants calculated for the two complexes are found to be 6.882 and 7.079 mdyn/Å. These values were then substituted into Jones relation [23]: $R_{U-O} = 1.08(F_{U-O})^{-1/3} + 1.17$. The values of R_{U-O} are found = 1.738 and 1.730 Å for the two complexes. The calculated F_{U-O} and R_{U-O} values fall in the usual range for the uranyl complexes [21].

3.1.4. Electronic spectra of H_4L^2 and its complexes

The UV spectrum of H_4L^2 showed bands at 48,540, 45,450, 43,470, 39,210, 36,496 and 34,483 cm^{-1} assigned to the $\pi \rightarrow \pi^*$ and $n \rightarrow \pi^*$ transitions of C=O, $C{=}N_{hydrazone}$ and $C{=}N_{oxime}$ [19].

The spectrum of the soluble part of $[ZrO(H_3L^2)(Cl)]_2{\cdot}2H_2O$ and $[HfO(H_3L^2)(Cl)]_2{\cdot}2H_2O$ in DMF showed bands at 35460, 33785, 26455, 24270, and 17005 cm^{-1} and 26520, 25779, 24330, 22220, and 21190 cm^{-1}. The bands at 35460 and 33784 cm^{-1} in the spectrum of $[ZrO(H_3L^2)(Cl)]_2{\cdot}2H_2O$ are assigned to the intraligand transitions while the other bands are due to LMCT transition [24], probably, $N \rightarrow Zr$ and $O \rightarrow Zr$. Scheme 2 represents the proposed structure for the dimmer form of the complex. The high melting points and the partial solubility confirm the dimmeric form.

In the electronic spectrum of $[UO_2(H_2L^2)]{\cdot}2H_2O$, the band at 22520 cm^{-1} is assigned to the $^1\Sigma g^+ \rightarrow {}^3\pi_4$ transition. This band is similar to the OUO symmetric stretching frequency for the first excited state [20]. Other bands at 28900, 26040 and 22520 cm^{-1} are assigned to intraligand and charge transfer transitions [25].

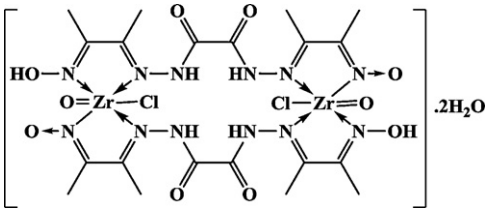

Scheme 2. Structure of $[ZrO(H_3L^2)(Cl)]_2{\cdot}2H_2O$.

Fig. 1. Biological effect of H2L1 and its complexes on the calf thymus DNA lanes arranged as: C—control DNA; 1—ligand; 2—UO_2^{2+}; 3—ZrO^{2+}; 4—Cr^{3+}.

3.2. Biological activity

3.2.1. Eukaryotic DNA degradation test

Examining the DNA degradation assay for H_4L^2 and H_2L^1 as well as their metal complexes revealed variability on their immediate damage on the calf thymus (CT) DNA. The complexes have a high effect on the calf thymus DNA than the ligands; HfO^{2+}, Cr^{3+} and ZrO^{2+} complexes of H_4L^2 degraded the CT DNA completely. The results suggest that direct contact of HfO^{2+} and ZrO^{2+} is necessary to degrade the DNA of Eukaryotic subject (Figs. 1 and 2).

3.2.2. Antibacterial activity

The ligands and their metal complexes were tested against Gram's positive Bacillus thuringiensis (BT) and Gram's negative bacteria (*E. coli*). All compounds have high inhibitory effects on Gram's positive bacteria; $[Cr(L^1)(Cl)(H_2O)_3]H_2O$ has the highest value giving zone diameter of 50 mm. The lowest one is H_2L. All compounds have small inhibitory effects on Gram's negative bacteria which can be attributed to the inability of the complexes to diffuse into the cell membrane of the organism. Examining the values for Gram's positive bacteria in Table 5, one can arrange the compounds as: $[Cr(L^1)(Cl)(H_2O)_3]H_2O > [HfO(H_3L^2)(Cl)]_2{\cdot}2H_2O > [UO_2(L^1)(EtOH)_2] > [ZrO(HL^1)_2]{\cdot}C_2H_5OH > [UO_2(H_2L^2)]_2{\cdot}2H_2O > [ZrO(H_3L^2)(Cl)]_2{\cdot}2H_2O \sim H_4L^2 > H_2L^1$.

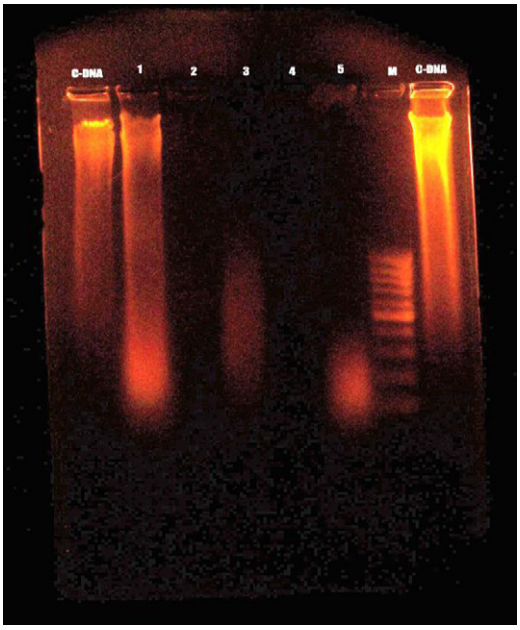

Fig. 2. Biological effect of H_4L^2 and its complexes on the calf thymus DNA Lanes arranged as: C—control DNA; 1—ligand; 2—VO^{2+}; 3—Cr^{3+}; 4—ZrO^{2+}.

3.3. Thermal analysis

The TGA thermogram of $[ZrO(HL^1)_2]\cdot C_2H_5OH$ showed the first step at 29–160 °C with a weight loss of 29.8% (calcd. 31.5) corresponding to the removal of $C_2H_5OH + ON_4H_4$. The second step ended at 355 °C with a weight loss of 22.5% (calcd. 20.7) corresponding to the evolution of C_4O_2. Thirdly, the removal of N_4H_6 is considered the last fragment of the ligand liberating in the temperature range 356–524 °C with a weight loss of 17.1% (calcd. 16.1). After which a constant weight was observed while ZrO_2 becomes the residual part with 29.5% (calcd. 31.8) weight loss.

$$[ZrO(C_4H_{10}N_8O_4)]\cdot C_2H_5OH$$

$$\rightarrow [ZrO(C_4H_4N_4O_4)] + \{C_2H_5OH + ON_4H_4\}$$

$$\rightarrow [ZrO(C_2O_4)] + \{C_4O_2\} \rightarrow ZrO_2 + \{N_4H_6\}$$

In the TGA thermogram of $[ZrO(H_3L^2)(Cl)]_2\cdot 2H_2O$, the first step (37–183 °C) representing the loss of $2H_2O + 4CH_3$ by a weight of 10.8% (calcd. 11.9). The second step at 184–450 °C representing the removal of $4CH_3 + C_4H_4N_4O_4 + Cl_2 + H_2O_2$ with a loss of 37.9% (calcd. 37.9). The third stage at 451–700 °C is attributed to the loss of 4C by 9.8% (calcd. 7.2). The residual part is $2ZrO_2N_4$ with a mass of 38.6% (calcd. 43.6).

$$[(ZrO)_2(C_{20}H_{30}N_{12}O_8Cl_2)]\cdot 2H_2O$$

Table 5
Antibacterial activities of the ligands and their complexes.

Compound (number)	Inhibition zone (mm)[a] Gram's positive bacteria (BT)
H_4L^2 (5)	18
$[ZrO(H_3L^2)(Cl)]_2\cdot 2H_2O$ (8)	18
$[HfO(H_3L^2)(Cl)]_2\cdot 2H_2O$ (6)	43
$[UO_2(H_2L^2)]_2\cdot 2H_2O$ (9)	23
H_2L^1 (1)	8
$[ZrO(HL^1)_2]\cdot C_2H_5OH$ (10)	28
$[Cr(L^1)(Cl)(H_2O)_3]H_2O$ (3)	50
$[UO_2(L^1)(EtOH)_2]$ (11)	39
Gentamicin	48

[a] Value for one record.

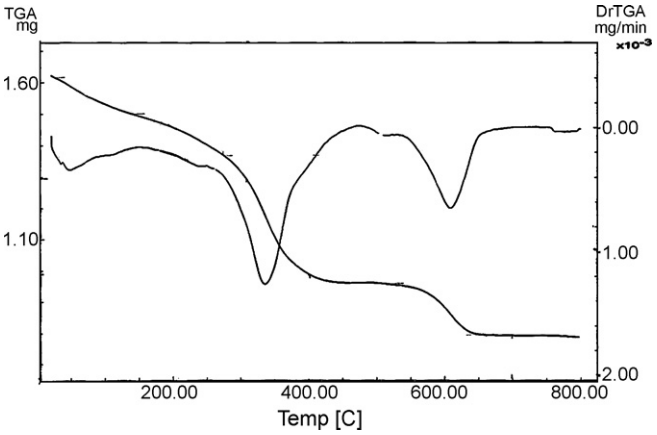

Fig. 3. Thermal analysis curves (TGA, DTA) of $[Cr(L^1)(Cl)(H_2O)_3]H_2O$.

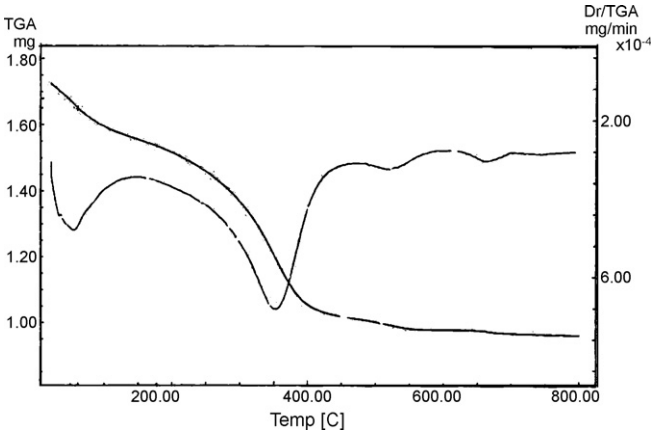

Fig. 4. Thermal analysis curves (TGA, DTA) of $[HfO(H_3L^2)(Cl)]_2\cdot 2H_2O$.

$$\rightarrow [(ZrO)_2(C_{16}H_{18}N_{12}O_8Cl_2)] + \{2H_2O + 4CH_3\}$$

$$\rightarrow (ZrO)_2(C_8N_8O_2) + \{4CH_3 + C_4N_4O_4H_4 + Cl_2 + H_2O_2\}$$

$$\rightarrow 2[ZrO_2N_4] + 4C$$

The TGA curve of $[Cr(L^1)(Cl)(H_2O)_3]H_2O$ (Fig. 3) showed the first stage ended at 140 °C representing the elimination of the hydrated water by 7.0% (calcd. 6.5). The second at 141–274 °C has 7.9% (calcd. 6.5) corresponding to the loss of one of the coordinated water molecule. The evolution of $½Cl_2 + 2H_2O$ occurred at 275–468 °C with 24.9% (calcd. 25.9). The last decomposition stage by 10.2% (calcd. 10.8) may be attributed to the loss of N_2H_2 at a temperature up to 658 °C. A steady stable region occurred at 659–800 °C referring to the residual part $[CrC_2H_2N_2O_2]$ having 41.9% (calcd. 41.9) weight loss.

$$[Cr(C_2H_4N_4O_2)Cl(H_2O)_3]H_2O$$

$$\rightarrow [Cr(C_2H_4N_4O_2)Cl(H_2O)_2] + \{H_2O\}$$

$$\rightarrow [Cr(C_2H_4N_4O_2)(H_2O)_2Cl] + H_2O$$

$$\rightarrow [Cr(C_2H_4N_4O_2)] + \{½Cl + 2H_2O\}$$

$$\rightarrow [CrO_2C_2N_2H_2] + \{N_2H_2\}.$$

The TGA curve of $[HfO(H_3L^2)Cl]_2.2H_2O$ (Fig. 4) displayed several decomposition stages. The first one ended at 144 °C is due to the elimination of $2H_2O + 4CH_3$ with weight loss of 8.6% (calcd. 8.7). The second step [found 30.7% (calcd. 30.7)] ended at 434 °C is due to the removal of $4CH_3 + C_4N_4O_4H_4 + Cl_2 + H_2O_2$. The third stage at 434–750 °C with weight loss of 2.9% (calcd. 2.7) is attributed to the

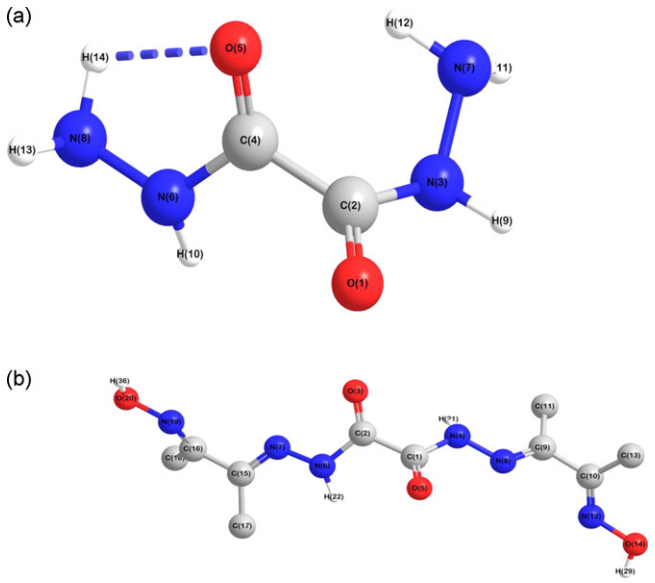

Scheme 3. Molecular modeling of H2L1 (a) and H4L2 (b).

loss of CN. Finally $\{2[HfO_2C_3N_3]\}$ is referred to the remaining part with 54.3% (calcd. 56.1) weight.

$$[(HfO)_2(C_{20}H_{30}N_{12}O_8Cl_2)]\cdot 2H_2O$$

$$\rightarrow [(HfO)_2(C_{16}H_{18}N_{12}O_8Cl_2)] + \{2H_2O + 4CH_3\}$$

$$\rightarrow (HfO)_2(C_8N_8O_2) + \{4CH_3 + C_4N_4O_4H_4 + Cl_2 + H_2O_2\}$$

$$\rightarrow 2[HfO_2C_3N_3] + CN$$

3.4. Molecular modeling of the ligands

The molecular parameters calculated for H_2L^1 (H_4L^2) are: total energy = −36016.23 (−82347.25), binding energy = −1193.24 (−3374.40), electronic energy = −153597.20 (−539181.59), heat of formation = −32.27 (84.37) kcal/mol, dipole moment = 1.81 (7.826) D, HOMO = −9.7720 (−9.5843) eV and LUMO = −0.1114 (−0.3313) eV. Scheme 3 represents their molecular modeling where the bond lengths and angles are recorded in Tables 1S and 2S.

In H_2L^1 modeling (Scheme 3a), a hydrogen bond is formed between the NH_2 and C=O groups from one side. No hydrogen bonding for the other two groups probably due to the distance is long. Also, the two carbonyl groups lie on different sides.

In H_4L^2 modeling (Scheme 3b), no hydrogen bonds due to the existence of each C=O and the adjacent NH in opposite sides. The distance between O(3) and H(22) is far enough to form bond. All bond angles were found between 100.8023 and 127.4972 confirming in most cases sp^2 and sp^3 hybridization.

4. Conclusion

Monomer, $[ZrO(HL^1)_2]\cdot C_2H_5OH$, $[Cr(L^1)(H_2O)_3Cl]H_2O$ and $[UO_2(L^1)(H_2O)_2]$ and dimmer, $[ZrO(H_3L^2)Cl]_2\cdot 2H_2O$, $[HfO(H_3L^2)Cl]_2\cdot 2H_2O$ and $[UO_2(H_2L^2)]\cdot 2H_2O$ complexes were isolated and characterized with oxalylhydrazide and oxalyl bis(diacetylmonoxime hydrazone). All have octahedral geometry and stable to thermal decomposition. Some complexes are decomposed immediately due to the presence of hydrated and coordinated water. All complexes have high activity towards calf thymus DNA than the ligands. They also have high inhibitory effect on Gram's positive than Gram's negative bacteria.

Appendix A. Supplementary data

Supplementary data associated with this article can be found, in the online version, at doi:10.1016/j.saa.2010.04.012.

References

[1] H.R. Maghler, E.H. Cordes, Biological Chemistry, Harper and Row, New York, 1971, p. 393;
H.M. Dawes, J.M. Waters, T.N. Waters, Inorg. Chim. Acta 66 (1982) 29.
[2] Z. Huszti, G. Szihigyi, E. Kasztreiner, Biochem. Pharmacol. 32 (1983) 627.
[3] S. Fucharoen, P.T. Rowley, N.W. Paul, Thalassemia: Pathophysiology and Management. Part B, Alan R. Liss, New York, 1998.
[4] L. Pickart, W.H. Goodwin, W. Burgua, T.B. Murphy, D.K. Johnson, Biochem. Pharmacol. 32 (1983) 3868.
[5] K.L. Bieda, A.L. Kranitz, J.J. Grzybwski, Inorg. Chem. 32 (1993) 4209.
[6] S. Gao, L.H. Huo, Z.P. Deng, H. Zhao, Acta Crystallogr. E 61 (2005) 152.
[7] S. Gao, L.H. Huo, J.W. Liu, C. Wang, J.G. Zhao, S.W. Ng, Acta Crystallogr. 644 (2004).
[8] Z.P. Deng, S. Gao, L.H. Huo, H. Zhao, Acta Crystallogr. 2214 (2005).
[9] A. Tolga, G. olak, H. Irez, T. Mutlu, H. kelek, N. Aylak, J. Coord. Chem. 62 (2009) 1005.
[10] W. Plass, A.S. El-Tabl, A. Pohlmann, J. Coord. Chem. 62 (2009) 358.
[11] A.A. El-Asmy, M.E. Khalifa, M.M. Hassanian, Ind. J. Chem. 43A (2004) 92.
[12] N.M. El-Metwally, A.A. Abou-Hussen, A.A. El-Asmy, IJPAC 1 (2006) 75.
[13] N. Nishat, S. Parveen, S. Dhyani Asma, J. Coord. Chem. 62 (2009) 1091.
[14] A.A. Adeniyi, K.S. Patel, Synth. React. Inorg. Met. Org. Chem. 26 (1996) 439.
[15] O.A. Al-Gammal, A.A. El-Asmy, J. Coord. Chem. 61 (2008) 2296.
[16] Z. Marczenko, Separation and Spectrophotometric Determination of Elements, John Wiley & Sons, Toronto, 1986.
[17] A.I. Vogel, A Text Book of Quantitative Inorganic Analysis, Longmans, London, 1994.
[18] N.M. El-Metwally, A.A. El-Asmy, J. Coord. Chem. 59 (2006) 1591.
[19] E.R. Price, J.R. Wasson, J. Inorg. Nucl. Chem. 36 (1974) 67.
[20] S.P. McGlynn, J.K. Smith, W.C. Neely, J. Mol. Spectrosc. 6 (1961) 164.
[21] A.Z. El-Sonbati, M.A. Diab, A.A. El-Asmy, Synth. React. Inorg. Org. Met. Chem. 19 (1989) 731.
[22] S.P. McGlynn, J.K. Smith, J. Chem. Phys. 35 (1961) 105.
[23] L.H. Jones, Spectrochim. Acta 10A (1958) 395.
[24] A.A. El-Asmy, M.A. Hafez, E.M. Saad, F.T. Taha, Transition Met. Chem. 19 (1994) 603.
[25] N.M. El-Metwally, R.M. El-Shazly, I.M. Gabr, A.A. El-Asmy, Spectrochim. Acta 61A (2005) 1113.